Using a Simple Crack Growth Model in Predicting Remaining Useful Life

Alexandra Coppe,* Matthew J. Pais,† Raphael T. Haftka,‡ and Nam H. Kim§
University of Florida, Gainesville, Florida 32611

The remaining useful life of a system can be predicted from available data and/or physical models, which is commonly known as prognosis. In this paper, the remaining useful life (e.g., the number of cycles to failure) of a system experiencing fatigue crack growth is estimated using a simple physical model. This paper shows that a simple model, such as the Paris model with an assumed analytical stress-intensity factor, can be used for complex geometries by compensating for the error in the assumed stress-intensity factor by adjusting model parameters. The adjustment is done automatically by a process of Bayesian identification. True damage growth is simulated using the extended finite-element method to model the effects of crack location and geometry on the relationship between crack size and stress-intensity factor. The detection process of crack size using structural health monitoring systems is modeled by adding random noise and a deterministic bias to the simulated damage growth. Equivalent model parameters are then identified using the Bayesian inference, from which the remaining useful life is estimated. Using three examples of damage geometries, it is shown that the remaining useful life estimates are accurate even with the use of an assumed analytical stress-intensity factor.

Nomenclature

a	=	current crack length
a_C	=	critical crack length
a_i	=	crack length at cycle N
a_o	=	initial crack length
b	=	bias applied to crack size data
C	=	Paris law constant
ΔK	=	stress-intensity factor range
K_{IC}	=	critical mode I stress-intensity factor
m	=	Paris law exponent

I. Introduction

FOR the last two decades, structural health monitoring (SHM) technology has been significantly developed such that it is feasible not only to detect damage but also to characterize the significance of damage [1,2]. In the case of structural damage due to cracks, SHM systems can now continuously monitor the growth of cracks during the lifecycle of an aircraft. When the data obtained from SHM results are incorporated with crack growth models, it is possible to predict the future behavior of damage. This is called model-based prognosis [3–5], which gives valuable information in terms of providing safety of aircraft and estimating appropriate maintenance schedules.

Although the model-based prognosis can be a powerful technology, it has the drawback that it often requires expensive computations. For example, Paris and Erdogan's model [6] describes the rate of crack growth as a function of stress-intensity factor. The stress-intensity factor is a complicated function of applied loading,

boundary conditions, crack position, and geometry. Except for simple geometries, numerical techniques such as finite-element analysis are required to calculate accurate stress-intensity factor [7–9]. This can cause a significant computational difficulty, because the statistical nature of prognosis requires evaluations of stress-intensity factor for numerous damage sizes.

The objective of this paper is to demonstrate that one can use simple models to predict the remaining useful life (RUL) even if the model has substantial errors. This is accomplished through the identification of an equivalent damage growth parameter that compensates for the difference between the simple model and the true stress-intensity factor. Thus, even if the actual crack growth behavior is different from the one obtained with the analytical stress-intensity factor, Bayesian inference can identify equivalent damage growth parameters, different from the true ones, such that the model accurately predicts future damage growth behavior. In this paper, we consider a horizontal crack growth in a thin plate under mode I loading condition. Inclined cracks or mixed-mode loading condition will be considered in the future.

The damage growth is simulated using the extended finite-element method (XFEM) for calculating 'true' stress-intensity factors, and the Paris model is used to grow the crack. XFEM [10] and allows for discontinuities to be modeled independently of the finite-element mesh, which avoids costly remeshing as the crack grows. The stress-intensity factors, which are the driving force for crack growth, are calculated within the XFEM framework using the domain form of the contour integrals [11].

In practice, the actual damage sizes are measured using SHM systems in which onboard sensors and actuators are used to detect damage location and size. It is noted that estimating damage size is still in the active research area (see, for example, An et al. [12]). In this paper, instead of using actual measurement data, synthetic data are generated using random noise and deterministic bias. Although there are some SHM data available, synthetic data are valuable in a sense that various statistical analyses, such as confidence interval of RUL, can be performed. First, true values of the model parameters are assumed. Then, the true crack will grow according to the given model parameters, prescribed operating, and loading conditions by XFEM simulations. Thus, the true crack size at every measurement time is known. With the true crack size, the true remaining useful life is defined when the crack size reaches the critical crack size, which is predetermined. It is assumed that the measurement instruments may have a deterministic bias and random noise. These bias and noise are added to the true crack sizes, to generate the synthetic measured crack

*Research Assistant, Department of Mechanical and Aerospace Engineering; alex.coppe@ufl.edu.

†Graduate Student, Department of Mechanical and Aerospace Engineering; mpais@ufl.edu.

‡Distinguished Professor, Department of Mechanical and Aerospace Engineering; haftka@ufl.edu.

§Associate Professor, Department of Mechanical and Aerospace Engineering; nkim@ufl.edu.

sizes. Then, these data are used to predict the equivalent damage growth parameters and thus the RUL. In this way, it is possible to evaluate the accuracy of prognosis method.

Of the many methods available for parameter identification, Bayesian inference [13] is used to identify damage growth parameters. This method is used to identify a probability distribution for model parameters. The identified distribution of damage growth parameters can then be used to predict the distribution of RUL.

The paper is organized into the following sections. In Sec. II, the crack growth model is introduced along with the notion of equivalent model parameter. In Sec. III, the model for measurement uncertainty that is used in this paper is explained. The Bayesian method is summarized in Sec. IV. Three numerical examples with increasing difference between the simple and true stress-intensity factor models are presented in Sec. V, followed by concluding remarks and future work in Sec. VI.

II.   Crack Growth Model

A crack in a plate can grow due to repeated application of stress. For example, a crack in a fuselage panel of aircraft can grow due to repeated pressurization cycles. In this paper, the original Paris model [6] is used to predict the crack growth in an infinite plate. In this model, the range of stress-intensity factor ΔK is the main factor driving the crack growth with two parameters, C and m, as

$$\frac{\mathrm{d}a}{\mathrm{d}N} = C(\Delta K)^m \tag{1}$$

where a is the characteristic crack size, and N is the number of fatigue loading cycles. The range of stress-intensity factor is calculated by the difference between maximum and minimum stress-intensity factors (i.e., $\Delta K = K_{\max} - K_{\min}$). Although the number of cycles is an integer, it is considered a real number as the crack grows over a great number of cycles. The two parameters, C and m, are usually estimated from experiments. When a log–log scale plot is made for the growth rate versus the stress-intensity factor, the slope corresponds to m, whereas the y intercept at $\Delta K = 1$ corresponds to C.

The simplest form of the stress-intensity factor is for mode I propagation in an infinite plate. In this case, the 'analytical' stress-intensity factor can be calculated as

$$\Delta K = \Delta\sigma\sqrt{\pi a} \tag{2}$$

where $\Delta\sigma$ is the range of applied nominal stress (i.e., stress far from the crack tip). By substituting Eq. (2) into Eq. (1), the differential equation can be solved for the crack size as a function of the number of cycles N_i as

$$a_i = \left[N_i C \left(1 - \frac{m}{2}\right)(\Delta\sigma\sqrt{\pi})^m + a_0^{1-\frac{m}{2}} \right]^{\frac{2}{2-m}} \tag{3}$$

where a_0 is the initial crack size. Note that the initial crack size does not have to be the size of the initial micro-crack in the pristine plate. When an SHM system is used, a_0 can be the size of crack that is initially detected. Then, Eq. (3) can be used to predict the crack size a_i after N_i cycles, starting from a crack with size a_0, assuming that the parameters C and m are known.

Considering Eq. (3) can calculate the crack size for any given number of cycles, it is also possible to calculate the required number of cycles for a crack to grow to a certain size. It is important to estimate how many cycles remain before failure. In general, a critical crack size a_C is defined in which the crack grows rapidly and becomes unstable. Then, starting from the current crack size (let us say that it is a_i), the remaining cycles until the crack grows to the critical crack size can be calculated by

$$N_f = \frac{a_C^{1-\frac{m}{2}} - a_i^{1-\frac{m}{2}}}{C(1-\frac{m}{2})(\Delta\sigma\sqrt{\pi})} \tag{4}$$

In SHM, Eq. (4) can be used to predict the RUL before the crack needs to be repaired. Again, the prediction process requires the two Paris parameters.

In general, the accuracy of Eq. (2) depends on geometrical effects, boundary conditions, crack shape, and crack location. A more general expression [7,8] of the range of stress-intensity factor can be written as

$$\Delta K' = Y\Delta K \tag{5}$$

where Y is the correction factor, given as the ratio of the true stress-intensity factor to the value predicted by Eq. (2). The correction factor depends on the geometry of the crack and plate and the loading conditions. Examples of the dependence of the correction factor on the crack size are shown in Fig. 1 for a center crack in an infinite plate, a center crack in a finite plate, and an edge crack in a finite plate [7,8]. Many advanced models are also available that can consider the effect of crack tip plasticity as well as the effect of crack closure [14–16]. The advanced models normally come with more parameters that need to be identified.

By comparing Eqs. (1), (2), and (5), an interesting and critically important observation can be made. For example, it is possible to use the range of stress-intensity factor in Eq. (2) instead of the one in Eq. (5) for the crack in a finite plate (i.e., it is possible to move the correction factor into the two Paris parameters). In such a case, the crack growth model in Eq. (1) can be modified as

$$\frac{\mathrm{d}a}{\mathrm{d}N} = C(\Delta K')^m \approx C'(\Delta K)^{m'} \tag{6}$$

where C' and m' are 'equivalent' Paris parameters for using the stress-intensity factor in Eq. (2). In the viewpoint of Eq. (6), it is possible to interpret the two Paris parameters as curve-fitting parameters, not material properties. This observation is consistent with the fact that the Paris parameters become different when the load ratio $R = K_{\min}/K_{\max}$ varies even if ΔK is the same [17]. The critical advantage of this viewpoint is that instead of using more complex models for crack growth for SHM prognosis, the simple model in Eq. (6) can be used as long as the equivalent parameters can be identified. In the numerical example section, this concept will be tested using various examples. From now on, notation has been changed such that C and m are used for equivalent parameters (C' and m'), while C_{true} and m_{true} are used for the original Paris model parameters.

For complex geometries with combined loadings, analytical expressions as given in Eqs. (2) and (5) may not be sufficient. For example, when a crack changes its path, the analytical growth rate equations cannot predict the correct path and growth of the crack. In such a case, a numerical method can be used to calculate the stress-intensity factor as well as the direction of crack growth. In this paper, XFEM is used to calculate the stress-intensity factor ΔK for complex geometry and loadings, and Eq. (6) is used to numerically integrate the crack size as a function of the number of cycles, which is explained in the Appendix.
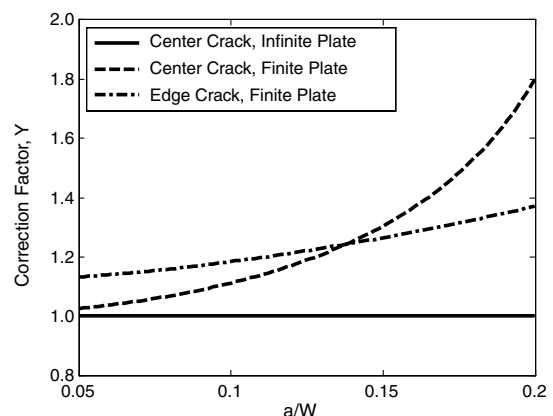

Fig. 1   **Correction factors for several plate geometries and crack sizes for a plate width of 200 mm.**

III. Measurement Uncertainty Model

The crack growth model in the previous section can be a powerful tool in maintaining the safety of a system and optimizing the maintenance schedule. However, the usefulness of the method depends on the accuracy of the parameters. For example, a 10% error in the exponent, m, can cause more than 100% difference in the predicted RUL from Eq. (4). Therefore, it is critical to accurately estimate these parameters. However, challenges exist when these parameters are measured from laboratory experiments: 1) the variability in different batches of materials is too large to make accurate and useful predictions, and 2) different loading and boundary conditions of practical panels affect these parameters. The premise of SHM is that frequently measured crack sizes can be used to identify 'panel-specific' damage growth parameters under given loading and boundary conditions, which is the main purpose of this paper. Then, these parameters can be used to predict the RUL before which the crack should be repaired.

Although there are some SHM data available, synthetic data are valuable in a sense that various statistical analyses, such as confidence interval of RUL, can be performed. In synthetic data, crack sizes are simulated and assumed to have been measured by SHM. In general, the crack sizes measured from SHM systems include the effect of bias and noise of sensor signals. The former is deterministic and represents a systematic departure caused by calibration error, while the latter is random and represents a noise in the signal. The synthetic measurement data are generated by 1) assuming that the true parameters, m_{true} and C_{true}, are known; 2) calculating the true crack growth, a_i^{true}, using the crack growth model in the previous section for a given N_i; and 3) adding a deterministic bias and random noise.

Let a_i^{true} be the true half-crack size at cycle N_i, b be the bias, and v be the noise. The measured half-crack size a_i^{meas} is then generated from

$$2a_i^{\text{meas}} = 2a_i^{\text{true}} + b + v \tag{7}$$

For subsequent measurements, the bias b remains constant, whereas the noise v is assumed to be normally distributed with mean 0 and standard deviation V, i.e., $v \sim N(0, V)$. It is noted that the current assumption on bias and noise is for convenience. In general, it is possible that the bias can vary as a function of time. Under the given models of bias and noise, the measured half-crack sizes are normally distributed as

$$a_i^{\text{meas}} \sim N\left(a_i^{\text{true}} + \frac{b}{2}, \frac{V}{2}\right) \tag{8}$$

Once the synthetic measurement data are generated, the true half-crack size a_i^{true} is not used any further, nor are the true values of parameters m_{true} and C_{true}. The questions that need to be addressed are as follows.
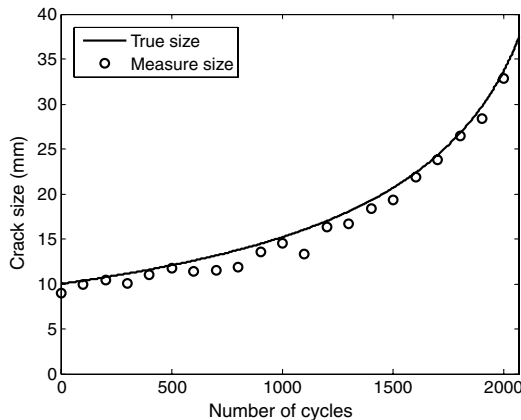

Fig. 2 Measured crack size at every 100 cycles with noise and bias compared to actual crack size (center crack in an infinite plate).

1) Is it possible to accurately estimate the two parameters using the synthetic data that have bias and noise?

2) What happens if different geometry or boundary conditions are used for the actual panel?

Figure 2 shows the measured crack sizes at every 100 cycles with a deterministic bias of $b = -2.0$ mm and normally distributed noise with mean 0 and standard deviation $V = 1.0$ mm. Note that, due to the bias, the trend of data is shifted from the true crack growth curve.

IV. Bayesian Method

Bayesian inference (e.g., Gelman et al. [18]) is often used for identifying unknown model parameters from data; it progressively improves the knowledge on the parameters using data, starting from the initial knowledge. Bayesian inference is able to incorporate the initial knowledge of the parameters and statistically identifies model parameters.

In estimating the RUL, the statistical information of parameters is important because a conservative estimate is required for the maintenance schedule. Bayesian inference is used to estimate the distribution of Paris model parameters, from which the distribution of the RUL is estimated.

Bayesian inference is based on Bayes's theorem on conditional probability [19]. It is used to obtain the updated (also called posterior) probability of a random variable by using new information. In this paper, it is used to improve the statistical distribution of unknown parameter m using SHM measured crack size a; indeed, this is the same as a_N^{meas} in Eq. (8). Therefore, the Bayes theorem is extended to the continuous probability distribution with probability density function (PDF), which is more appropriate for the purpose of the present paper. Let $f_X(m)$ be a PDF of Paris model parameter $X = m$. The measured crack size $Y = a$ is also random due to the noise, whose PDF is denoted by $f_Y(a)$. Then, the joint PDF of X and Y can be written in terms of f_X and f_Y, as

$$f_{XY}(m, a) = f_X(m|Y = a)f_Y(a) = f_Y(a|X = m)f_X(m) \tag{9}$$

When X and Y are independent, the joint PDF can be written as $f_{XY}(m, a) = f_X(m) \cdot f_Y(a)$, and Bayesian inference cannot be used to improve $f_X(m)$. Using the aforementioned identity, the original Bayes theorem can be extended to the PDF form as [20,21]

$$f_X(m|Y = a) = \frac{f_Y(a|X = m)f_X(m)}{f_Y(a)} \tag{10}$$

Because the integral of $f_X(m|Y = a)$ should be 1, the denominator in Eq. (10) can be considered as a normalizing constant. In Eq. (10), $f_X(m|Y = a)$ is the posterior PDF of Paris model parameter given measured crack size $Y = a$, and $f_Y(a|X = m)$ is the likelihood function or the PDF value of obtaining the measured crack size a for a given parameter value of $X = m$.

When the analytical expressions of the likelihood function $f_Y(a|X = m)$ and the prior PDF $f_X(m)$ are available, the posterior PDF in Eq. (10) can be obtained through simple calculation. The likelihood function is designed to integrate the information obtained from SHM measurement to the knowledge about the distribution of m. Instead of assuming an analytical form of the likelihood function, uncertainty in measured crack sizes is propagated and estimated using the Monte Carlo simulation (MCS). Although this process is computationally expensive, it will provide accurate information for the posterior distribution. The derivation of the likelihood function can be found in Coppe et al. [4].

An important advantage of Bayes's theorem over other parameter identification methods, such as the least square method and maximum likelihood estimate, is its capability to estimate the uncertainty structure of the identified parameters. These uncertainty structures depend on that of the prior distribution and likelihood function. Accordingly, the accuracy of posterior distribution is directly related to that of likelihood and prior distribution. Thus, the uncertainty in posterior distribution must be interpreted in that context.

Although the two parameters C and m need to be identified, in this paper it is assumed that the value of C_{true} is given, and m is the only unknown for the sake of simplicity in explanation. Bayesian inference for updating joint PDF of multiple parameters can be found in An et al. [22]. Bayesian inference uses data at every 100 cycles to make the interval coincide with A-checks of the airplane (i.e., a small maintenance task carried out overnight at the airliner's hub hangars). In addition, too-frequent measurement may not obtain valuable information because cracks grow slowly.

There are different ways of representing the posterior distribution from Bayesian inference, such as Markov-chain Monte Carlo or the grid method. In this paper, the latter is employed. The prior distribution of m is assumed to be uniform between 3.3 and 4.3 initially. This range is then divided into 200 intervals, and the values of PDF in Eq. (10) are evaluated at each interval; the PDF is approximated by piecewise linear polynomial.

Once the distribution of m is identified at a given cycle N_i, it can be used to calculate the distribution of RUL N_f using Eq. (4). The distribution of RUL represents the possibility of remaining cycles before the crack size becomes the critical one. In this paper, the critical crack size is defined as $a_C = 24$ mm. This is different from the conventional definition of critical crack size, which depends on the fracture toughness. Rather, it is a threshold of crack size that an airline company may want to repair the crack.

Because the updated distribution of m does not follow any analytical distribution, MCS is used to estimate the distribution of RUL. In addition, the measured crack size is also randomly distributed according to Eq. (8). From the RUL distribution, the fifth percentile is used as a conservative estimate of RUL. Therefore, the estimated RUL will be less than the true RUL with a 95% confidence.

An important advantage of using synthetic data is that it allows predicting the statistical characteristic of predicted results. In this paper, random noises are added to the true crack sizes. Due to this randomness, different RUL distributions are expected if another set of synthetic data is used. The same will happen during actual experiments. Therefore, to cover actual experimental variability, the process of identifying damage parameters and predicting the conservative RUL is repeated 100 times with different sets of synthetic data. In the numerical examples, 68% confidence interval of fifth percentiles is plotted, which corresponds to mean ± one standard deviation.

V. Numerical Examples

In this section, three numerical examples are presented in the order of increasing difference between the true and assumed stress-intensity factor model. For all examples, an aluminum 7075 square plate with dimension of 0.2×0.2 m and thickness of 248 mm is used with Young's modulus $E = 71.7$ GPa, Poisson's ratio $\nu = 0.33$, and Paris model parameters $C_{\text{true}} = 1.5 \times 10^{-10}$ and $m_{\text{true}} = 3.8$. Mode I

fatigue loading is applied to the plate with the range of stress $\Delta\sigma = 78.6$ MPa ($\sigma_{\max} = 78.6$, $\sigma_{\min} = 0$), which corresponds to the case of fuselage pressurization loading. The relatively large initial crack size $a_0 = 10$ mm is chosen because many SHM sensors cannot detect small cracks. In addition, there is no significant crack growth when the size is small. This size of crack is still too small to threaten the safety of aircraft.

'True' crack growth data were calculated using XFEM simulations, which were performed on a structured mesh of square linear quadrilateral elements with characteristic length of 1 mm. Each cycle of fatigue crack growth was modeled until the half-crack size reaches a threshold size of 24 mm (i.e., the crack will be repaired beyond this size). Synthetic measurement data are then generated by adding a deterministic bias and random noise to the true crack size according to Eq. (8). The crack size at each iteration was then used to identify the equivalent Paris model exponent through the use of the Bayesian inference with the simplified stress-intensity formula in Eq. (2). Last, the RUL is estimated as the number of remaining cycles that the current crack size reaches the threshold one.

A. Center Crack in a Finite Plate

The first example considered is that of a center crack in a finite plate, as shown in Fig. 3a. Only the right half of the plate was modeled with XFEM through the use of symmetry. The corresponding curve of the correction factor Y for the center crack in a finite plate is given in Fig. 3b. The accuracy of the correction factor calculated from XFEM is presented in the Appendix. In this example, it is clear that the effect of the correction factor is less than 5%. Therefore, it is expected that the identification of damage growth parameter will be close to the true one.

The crack growth went up to 1600 cycles, and the crack size at 1700 cycles becomes larger than the threshold size. Figure 4a shows the updated distribution of m using Bayesian inference at 1600 cycles using a single set of measurements. The initial distribution was assumed to be uniformly distributed (i.e., $m \sim U[3.3; 4.3]$). The standard deviation at the final update turns out to be about 0.015, which is significantly reduced from the initial value of 0.29. For comparison, the true value, m_{true}, is also shown as a vertical dashed line. Although the true crack grows according to the range of stress-intensity factor in Eq. (5), Bayesian inference assumes that it is given in Eq. (2). The maximum likelihood value, 3.85, slightly overestimates the true one to compensate for the error in ΔK. This is expected because the correction factor is slightly larger than one, which makes the crack grow faster than it would if it was in an infinite plate. Figure 4b shows the 68% confidence interval of crack size obtained using the identified parameter m. The 68% confidence interval of m (e.g., 3.83 and 3.86 in Fig. 4a) is used as an input into Eq. (3) to calculate the confidence interval of crack lengths to the cycle of the last Bayesian identification. For comparison, the true
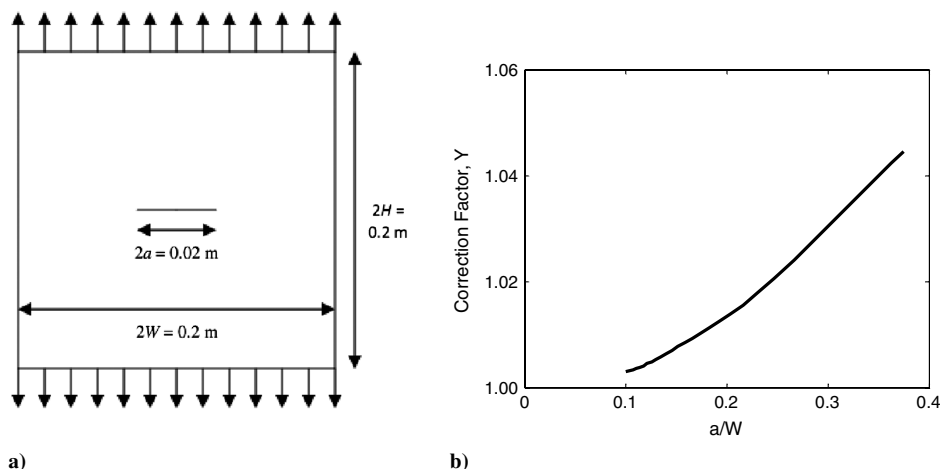

Fig. 3 Center crack in a finite plate model and correction factor: a) initial crack geometry and loading condition, and b) correction factor as a function of crack size.
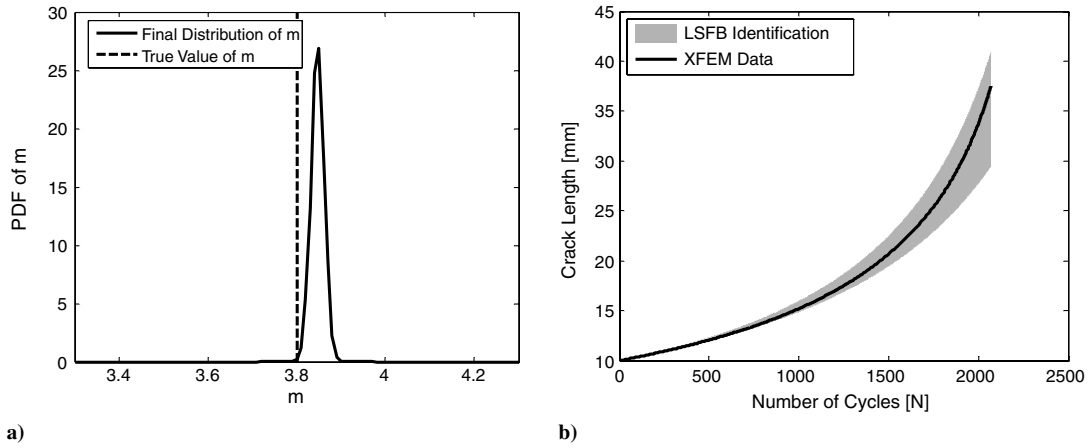
Fig. 4 Distribution of parameter *m* and crack growth from Bayesian inference using a single set of measurement data for a center crack in a finite plate: a) updated PDF of parameter m at cycle 1,600, and b) 68% confidence interval of crack growth.

crack sizes calculated from XFEM is plotted with a solid curve. It is noted that the true crack sizes (black line) fall within the bounds of the Bayesian identification (gray region).

Figure 5a shows the fifth-percentile conservative estimates of RUL. The black solid line represents the true RUL; it starts with 1600 because the crack will grow to the threshold size after 1600 cycles from the first detection. The true RUL is calculated using the range of stress-intensity factor in Eq. (5). In the same plot, the dashed line is the estimated RUL when the correction factor is assumed to be $Y = 1$; i.e., the range of stress-intensity factor is calculated using Eq. (2). Due to the slight underestimate of correction factor, the dashed RUL is also slightly higher than the true one, which is an unconservative estimate. However, both RULs eventually meet toward the end of life. Both lines use the information of true parameter m_{true}. The gray area in Fig. 5a represents the 68% confidence interval (mean ± standard deviation) of the estimated RUL using Bayesian inference. It can be observed that the estimate of RUL converges to the true RUL from the conservative side. It is noted that, even if Eq. (2) is used, the error in the stress-intensity factor is compensated by identifying equivalent parameter m that is slightly larger than the true one.

Figure 5b shows the 68% confidence interval of the relative accuracy (RA) [23] of the maximum estimation of the estimated RUL distribution N_f^{max} with respect to the true RUL N_f^{true}, defined as

$$\text{RA}_f = \frac{|N_f^{\text{true}} - N_f^{\text{max}}|}{N_f^{\text{true}}} \quad (11)$$

It can be observed the relative error gradually decreases due to better identification as more data are used in the Bayesian process.

However, the relative error increases at the last cycle because the denominator in Eq. (11) becomes small.

B. Edge Crack in a Finite Plate

Next, an edge crack in a finite plate is considered as shown in Fig. 6a. For this case, the boundary conditions were fixing the lower right-hand corner and allowing the top-right corner to only move in the vertical direction. It was found that the threshold crack size was reached at 955 cycles. Therefore, Bayesian inference was applied only nine times (one at every 100 cycles). The correction factor corresponding to the finite effect that this edge crack represented is given in Fig. 6b. In this case, the correction factor can contribute up to 35% to the stress-intensity factor. Therefore, it is expected that the equivalent damage growth parameter m will overestimate the true one in proportion.

Figure 7a shows the updated distribution of m using Bayesian inference at 900 cycles after the first detection. As expected, it compensates for the error in ΔK by overestimating m by 5.5%. It can be observed that the more the error in ΔK increases, the more m is overestimated to compensate for the error. That is, the model error due to not including the correction factor in ΔK calculation is compensated by overestimating m. The standard deviation of the final distribution of m is about 0.02, which is wider than the case of a center crack in an infinite plate. This is probably caused by the increased difference between the actual and assumed models for the stress-intensity factor.

As Bayesian inference results in a final distribution of m, the predicted crack sizes with this distribution are plotted and compared directly to the XFEM data in Fig. 7b. The XFEM data fall within the bounds of the Bayesian inference identification. It can be seen that
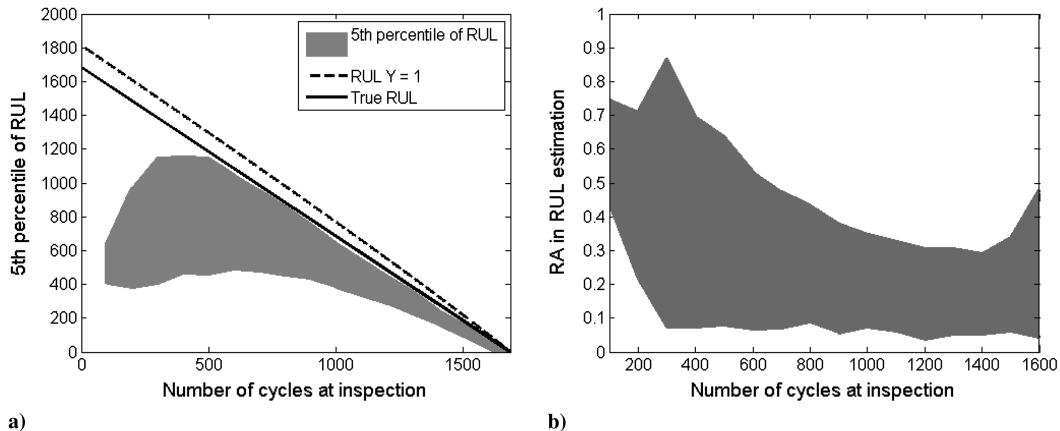

Fig. 5 Estimated RUL and relative accuracy [Eq. (11)] for a center crack in a finite plate: a) 68% confidence interval of fifth-percentile conservative RUL estimates, and b) 68% confidence interval of RA of the maximum likelihood of the estimated RUL distribution with respect to the true RUL.
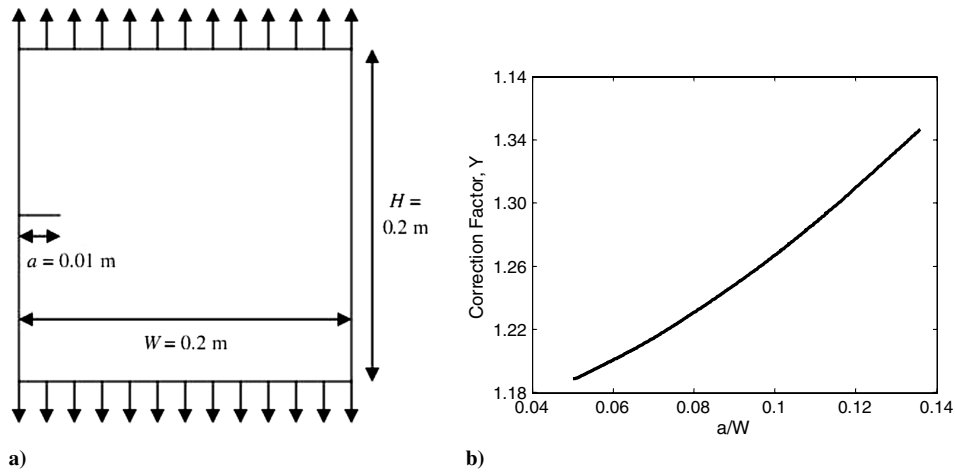
Fig. 6   Edge crack in a finite-plate model and the correction factor: a) initial crack geometry, and b) correction factor as a function of crack size.
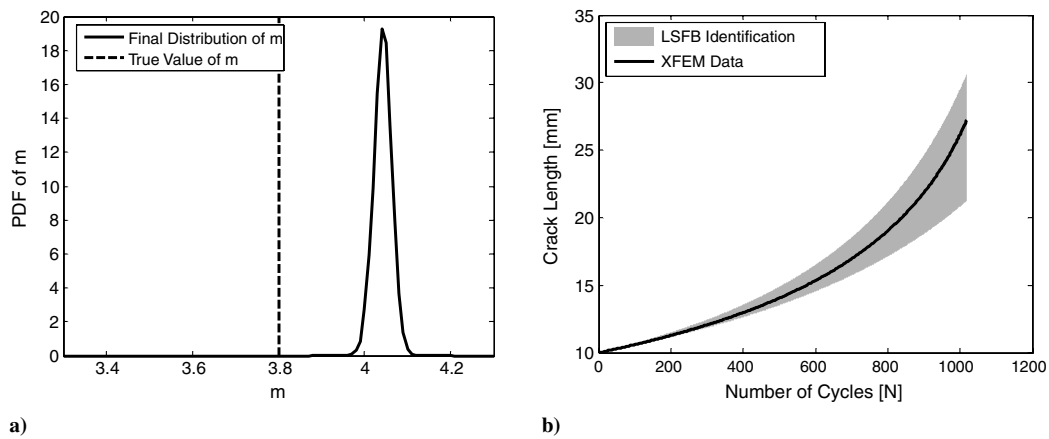

Fig. 7   Comparison of XFEM crack growth data with crack growth predicted from Bayesian inference for edge crack: a) updated PDF of parameter _m_ at cycle 900, and b) distribution of identified crack size (68% confidence interval).

the Bayesian process can compensate for the increase in the correction factor by gradually increasing the Paris model parameter. In that sense, the Paris model parameters are not considered as material properties. Rather, they are extrapolation parameters to match the crack growth trend.

Figure 8a shows the fifth-percentile conservative estimates of RUL, similar to Fig. 5a. In this case, there was a large difference between the true RUL and the RUL with $Y = 1$ assumption. The error of up to 35% in the correction factor leads to an overestimation in the RUL of almost 100%. However, both RULs eventually managed to meet toward the end of life. Even if the RUL with $Y = 1$ leads to a large overestimation, the 68% confidence interval of the conservative estimated RUL using Bayesian inference (gray area) stays in the conservative side and converges to the true RUL. Again, the large error in the correction factor has successfully been compensated by identifying equivalent parameter m that is about 5.5% larger than the true one.

Figure 8b shows the RA of the maximum likelihood of the estimated distribution of the RUL with respect to the true RUL. As observed previously, accuracy increases as more information is
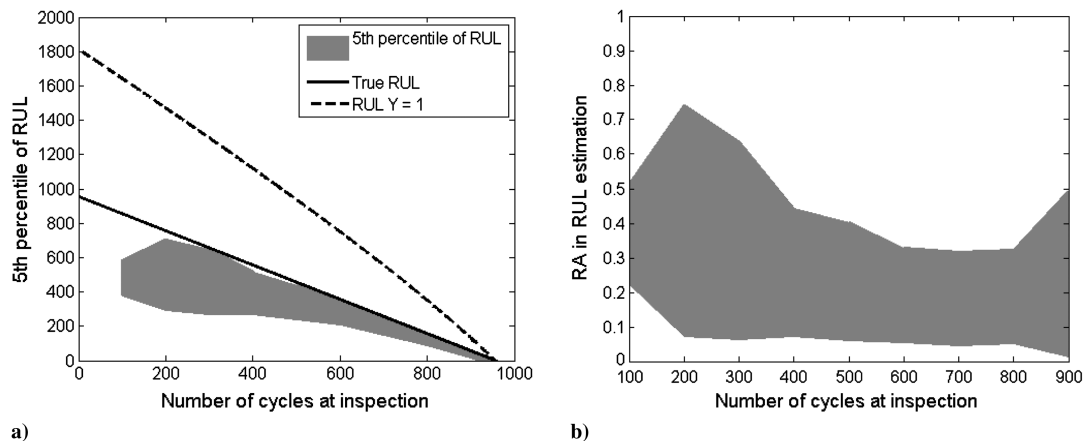

Fig. 8   Estimated RUL and relative accuracy [Eq. (11)] for an edge crack in a finite plate: a) 68% confidence interval of fifth-percentile conservative RUL estimates, and b) 68% confidence interval of RA of the maximum likelihood of the estimated RUL distribution with respect to true RUL.
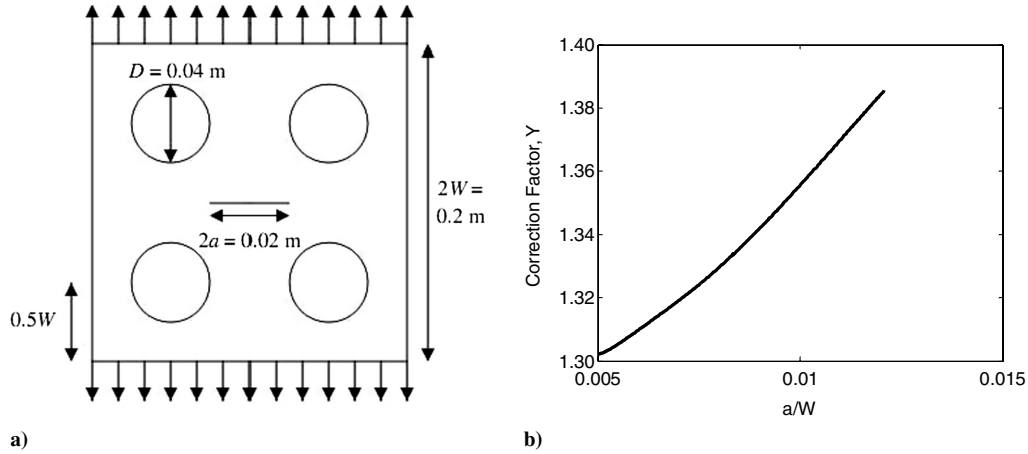
Fig. 9 Center crack in a finite plate with holes and the correction factor: a) initial crack geometry, and b) correction factor as a function of crack size.

available, the standard deviation decreases as well except for the last inspection (less than 100 cycles from failure).

C. Center Crack in a Plate with Holes

The final example considers differences between the actual and predicted model that may be caused by localized stress concentrations in the plate. Four holes are inserted into the plate, as shown in Fig. 9a. Only the right half of the plate was modeled with XFEM through the use of symmetry. Different from the two previous examples, there is no analytical expression of the correction factor; therefore, it is obtained from XFEM, as shown in Fig. 9b. The effect of holes is converted into 30–39% error in the stress-intensity factor. Due to such a large stress-intensity factor, the crack grew fast and reached the threshold size at 625 cycles. Therefore, only six updates were available for the Bayesian inference.

Figure 10a shows the updated distribution of m using Bayesian inference at cycle 600. As expected, it compensates for the error in ΔK by overestimating m by 8.7%. The same conclusion as before can be drawn: the larger the error in ΔK, the more m is overestimated
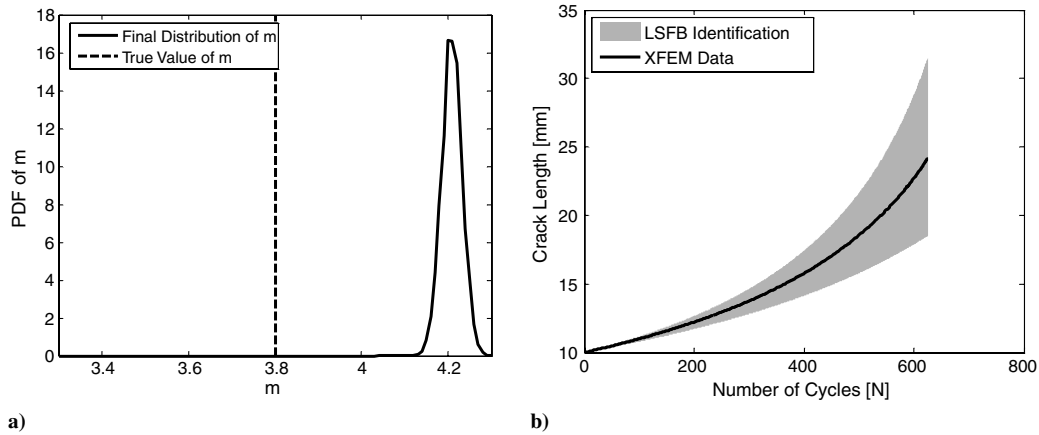

Fig. 10 Comparison of XFEM crack growth data with crack growth predicted from Bayesian inference for a plate with holes: a) updated PDF of parameter m at cycle 600, and b) distribution of identified crack size (68% confidence interval).
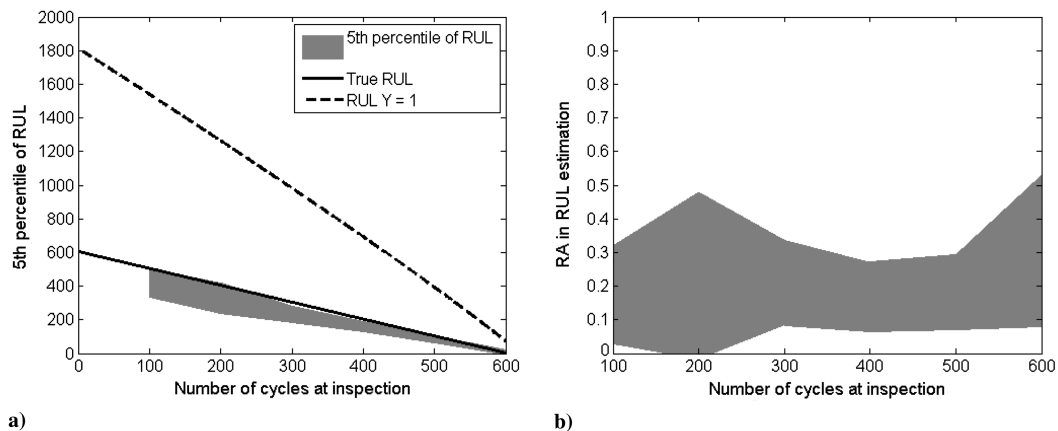

Fig. 11 Estimated RUL and relative accuracy [Eq. (11)] for a plate with holes: a) 68% confidence interval of fifth-percentile conservative RUL estimates, and b) 68% confidence interval of RA of the maximum likelihood of the estimated RUL distribution with respect to the true RUL.

to compensate for it. Due to this error, the standard deviation of m becomes about 0.024, which is still a significant reduction from the initial standard deviation of 0.29.

As the Bayesian inference results in a final distribution of m, the predicted crack lengths for this distribution are plotted and compared directly to the XFEM data in Fig. 10b. The XFEM data fall within the bounds of the Bayesian inference identification. The identified crack size distribution is wider than the previous two examples, which is because the model is increasingly far away from the center crack in an infinite-plate mode. In addition, the fact that only six inspections have been performed before reaching the threshold may also contribute to the relatively wide distribution.

Figure 11a shows the fifth-percentile conservative estimates of RUL, similar to Fig. 5a. Because there is no analytical approximation of correction factor is available, only the true RUL and the 68% confidence interval of the conservative estimated RUL using Bayesian inference (gray area) are plotted. Note that the predicted RUL stays close to the true one from the conservative side. Again, the large error in the correction factor has successfully been compensated by identifying equivalent parameter m that is about 8.7% larger than the true one.

Figure 11b shows the RA of the maximum likelihood of the estimated distribution of the RUL with respect to the true RUL. As observed previously, despite the fact that a simplistic model is used in which the range of stress-intensity factor does not account for the complexity of the geometry, Bayesian inference was able to estimate the RUL. The accuracy increases as more data is available except in this case as well for the last inspection. It has to be noted that the accuracy is similar in amplitude to the previous cases despite the modeling error being larger.

VI.   Conclusions

In this paper, equivalent damage growth parameters were identified, which can compensate for complex geometric effects for structural health monitoring prognosis. The error in stress-intensity factor was moved to the equivalent damage growth parameter, such that the prediction of remaining useful life is accurate. Three numerical examples showed that the deviation of damage growth parameter is proportional to the error in stress-intensity factor. All three examples, however, showed that the estimated conservative remaining useful life converges to the true one from the safe side. Therefore, it is concluded that a simple model can be used to predict the behavior of complex problems by calculating equivalent parameters.

Bayesian inference was proposed in identifying unknown model parameters. The method is demonstrated here updating only one parameter, m of the Paris model; the same idea can be applied to the parameters m and C together. This should allow for even more accurate results because it would allow for more flexibility in fitting the equivalent model.

Appendix: Extended Finite-Element Method

Modeling crack growth in a traditional finite-element framework is a challenging task because the domain of interest is defined by the mesh that needs to be continuously modified. At each increment of crack growth, at least the domain surrounding the crack tip must be re-meshed such that the updated crack geometry is accurately represented. If a large number of cycles are to be considered, this repeated remeshing can consume a large amount of the computational time for the analysis.

Extended finite-element method (XFEM) allows discontinuities to be represented independently of the finite-element mesh [10]. Arbitrarily oriented discontinuities can be modeled by enriching all elements cut by a discontinuity using enrichment functions satisfying the discontinuous behavior and additional nodal degrees of freedom. For the case of a domain containing a crack and voids [24], the approximation takes the following form:

$$u^h(x) = V(x) \sum_I N_I(x)[u_I + H(x)a_I + \sum_\alpha \Phi_\alpha(x)b_I^\alpha] \qquad (A1)$$

where $N_I(x)$ are the finite-element shape function; $V(x)$ is the void enrichment function; $H(x)$ is the Heaviside enrichment function; $\Phi_\alpha(x)$ are the crack tip enrichment functions; and u_I, a_I, and b_I^α are the classical and enriched degrees-of-freedom (DOFs). Equation (A1) is then used to build the stiffness matrix and solve for unknown DOFs. To decrease the computational time for the repeated solutions, an exact reanalysis algorithm [25] is used, which takes advantage of the large constant portion of the global stiffness matrix that does not vary according to crack growth.

The mixed-mode stress-intensity factors ΔK_I and ΔK_{II} for the given cracked geometry were calculated using the domain form of the interaction integrals [11]. The direction of crack growth was calculated using the maximum circumferential stress criterion [26]. The effective stress-intensity factor [27] given as

$$\Delta K_{\text{eff}} = \sqrt[4]{\Delta K_I^4 + 8\Delta K_{II}^4} \qquad (A2)$$

was used to convert the mixed-mode stress-intensity factors into a single value for used in the Paris model. The crack growth at each fatigue loading cycle is given as

$$\Delta a = C(\Delta K_{\text{eff}})^m \qquad (A3)$$

This is equivalent to the forward Euler method to integrate the differential Eq. (1). Then, the crack geometry is updated and the analysis moves on to the next loading cycle.

The implementation of XFEM used here was verified using the center crack in a finite plate given in Sec. III. For this problem the theoretical finite correction factor based on the equations of elasticity for a center crack in a finite plate [7,8] is given as
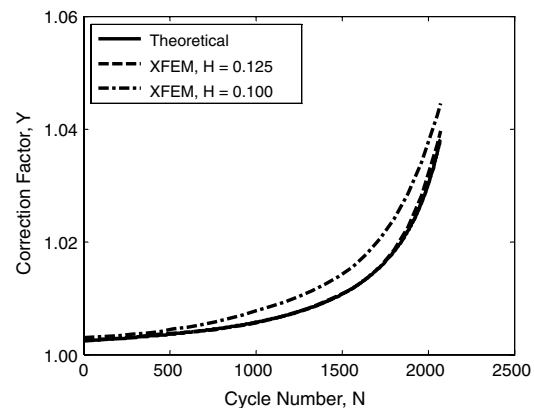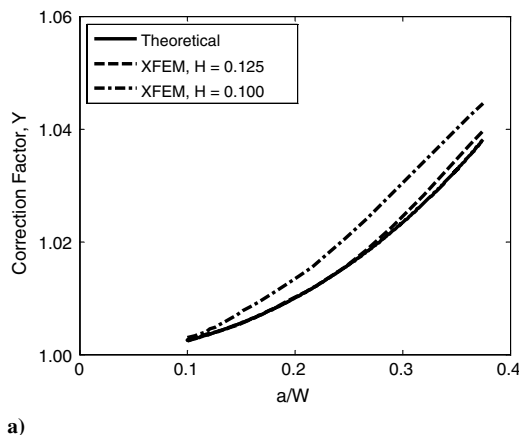

a)   b)

Fig. 12   Theoretical and XFEM predictions of correction factor for the center crack of a finite plate with different plate heights.

$$Y = \sqrt{\sec\left(\frac{\pi\lambda}{2}\right)\left(1 - \frac{\lambda^2}{40} + \frac{3\lambda^4}{50}\right)} \qquad (A4)$$

where $\lambda = a/W$, and a and W are the half-crack size and half-plate width. This model assumes that the plate is finite in the crack direction and infinite in the loading direction. A comparison of the crack lengths as a function of the number of cycles was first performed to ensure the accuracy of the XFEM data provided to the parameter identification routine. As there is no closed form solution for the crack size as a function of N due to the finite correction factor given in Eq. (5), the forward Euler method with 10,000 steps was used. This step size represents less than 0.1% change from 1000 steps. A comparison of the results is shown in Fig. 12 in which the correction factors are plotted with respect to a/W and the number of cycles. Because the theoretical correction factor in Eq. (A4) assumes that the plate is finite in the crack direction but infinitely long in the loading direction, the correction factor calculated from XFEM converges to the theoretical one when the height of plate increases.

Acknowledgments

References

[1] Giurgiutiu, V., *Structural Health Monitoring with Piezoelectric Wafer Active Sensors*, Academic Press, New York, 2008.

[2] Sohn, H., Farrar, C. R., Hemez, F. M., Czarnecki, J. J., Shunk, D. D., Stinemates, D. W., et al., "A Review of Structural Health Monitoring Literature: 1996–2001," Los Alamos National Laboratory Rept. LA-13976-MS, Los Alamos, NM, 2004.

[3] Papazian, J. M., Anagnostoua, E. L., Engela, S. J., Hoitsmaa, D., Madsena, J., Silbersteina, R. P., et al., "A Structural Integrity Prognosis System," *Engineering Fracture Mechanics*, Vol. 76, No. 5, 2009, pp. 620–632.
doi:10.1016/j.engfracmech.2008.09.007

[4] Coppe, A., Haftka, R. T., Kim, N. H., and Yuan, F. G., "Uncertainty Reduction of Damage Growth Properties Using Structural Health Monitoring," *Journal of Aircraft*, Vol. 47, No. 6, 2010, pp. 2030–2038.
doi:10.2514/1.C000279

[5] Orchard, M., and Vachtsevanos, G., "Particle Filtering Approach for On-Line Prognosis in a Planetary Carrier Plate," *International Journal of Fuzzy Logic and Intelligent Systems*, Vol. 7, No. 4, Dec. 2007, pp. 221–227.

[6] Paris, P., and Erdogan, F., "A Critical Analysis of Crack Propagation Laws," *Journal of Basic Engineering*, Vol. 85, 1963, pp. 528–534.
doi:10.1115/1.3656900

[7] Y. Murakami, (ed.) *Stress Intensity Factors Handbook*, Pergamon Press, New York, 1987.

[8] Tada, H., Paris, P., and Irwin G., *The Stress Analysis of Cracks Handbook*, American Society of Mechanical Engineers, Fairfield, NJ, 1987.

[9] Maligno, A. R., Rajaratnam, S., Leen, S. B., and Williams, E. J., "A Three-dimensional (3D) Numerical Study of Fatigue Crack Growth Using Remeshing Techniques," *Engineering Fracture Mechanics*, Vol. 77, No. 1, 2010, pp. 94–111.
doi:10.1016/j.engfracmech.2009.09.017

[10] Moës, N., Dolbow, J., and Belytschko, T., "A Finite Element Method for Crack Growth without Remeshing," *International Journal of Numerical Methods in Engineering*, Vol. 46, No. 1, 1999, pp. 131–150.

doi:10.1002/(SICI)1097-0207(19990910)46:1<131::AID-NME726>3.0.CO;2-J

[11] Shih, C., and Asaro, R., "Elastic-Plastic Analysis of Crack on Bimaterial Interface, Part 1: Small Scale Yield," *Journal of Applied Mechanics*, Vol. 55, No. 2, 1988, pp. 299–316.
doi:10.1115/1.3173676

[12] An, J., Haftka, R. T., Kim, N. H., Yuan, F. G., Kwak, B. M., Sohn, H., et al., "Experimental Study on Identifying Cracks of Increasing Size Using Ultrasonic Excitation," *Structural Health Monitoring*, Vol. 11, No. 1, 2012, pp. 95–108.

[13] Coppe, A., Haftka, R. T., and Kim, N. H., "Least Squares-Filtered Bayesian Updating for Remaining Useful Life Estimation," *51st AIAA/ASME/ASCE/AHS/ASC Structures, Structural Dynamics, and Materials Conference*, Orlando, FL, April 2010; also AIAA Paper 2010-2593.

[14] Beden, S., Abdullah, S., and Ariffin, A., "Review of Fatigue Crack Propagation Models in Metallics Components," *European Journal of Scientific Research*, Vol. 28, No. 3, 2009, pp. 364–397.

[15] Ibrahim, F. K., Thompson, J. C., and Topper, T. H., "A Study of Effect of Mechanical Variables on Fatigue Crack Closure and Propagation," *International Journal of Fatigue*, Vol. 8, No. 4, 1986, pp. 135–142.
doi:10.1016/0142-1123(86)90004-6

[16] Xiaoping, H., Moan, T., and Weicheng, C., "An Engineering Model of Fatigue Crack Growth Under Variable Amplitude Loading," *International Journal of Fatigue*, Vol. 30, No. 1, 2008, pp. 2–10.
doi:10.1016/j.ijfatigue.2007.03.004

[17] Sun, C. T., *Mechanics of Aircraft Structures*, 2nd ed., Wiley, New York, 2006.

[18] Gelman, A., Carlim, J. B., Stern, H. S., and Rubin, D. B., *Bayesian Data Analysis*, 2nd ed., Chapman & Hall/CRC, New York, 2004.

[19] Bayes, T., "An Essay Towards Solving a Problem in the Doctrine of Chances," *Philosophical Transactions of the Royal Society*, Vol. 53, 1763, pp. 370–418.

[20] Athanasios, P., *Probability, Random Variables, and Stochastic Processes*, 2nd ed., McGraw–Hill, New York, 1984.

[21] An, J., Acar, E., Haftka, R. T., Kim, N. H., Ifju, P. G., and Johnson, T. F., "Being Conservative with a Limited Number of Test Results," *Journal of Aircraft*, Vol. 45, No. 6, 2008, pp. 1969–1975.
doi:10.2514/1.35551

[22] An, D., Choi, J.-H., and Kim, N. H., "Identification of Correlated Damage Parameters Under Noise and Bias Using Bayesian Inference," *Structural Health Monitoring*, Vol. 11, No. 3, 2012, pp. 293–303.
10.1177/1475921711424520

[23] Saxena, A., Celaya, J., Saha, B., Saha, S., and Goebel, K., "On Applying the Prognostics Performance Metrics," *Annual Conference of the PHM Society*, Vol. 1, Prognostics and Health Management Society, San Diego, CA, 2009.

[24] Daux, C., Moës, N., Dolbow, J., Sukumar, N., and Belytschko, T., "Arbitrary Branched and Intersecting Cracks with the Extended Finite Element Method," *International Journal for Numerical Methods in Engineering*, Vol. 48, No. 12, 2000, pp. 1741–1760.
doi:10.1002/1097-0207(20000830)48:12<1741::AID-NME956>3.0.CO;2-L

[25] Pais, M., Yeralan, S. N., Davis, T. A., and Kim, N. H., "An Exact Reanalysis Algorithm Using Incremental Cholesky Factorization and Its Application to Crack Growth Modeling," *International Journal for Numerical Methods in Engineering*, 2012 (published online).
10.1002/nme.4333

[26] Erdogan, F., and Sih, G. C., "On the Crack Extension in Plates Under Plane Loading and Transverse Shear," *Journal of Basic Engineering*, Vol. 85, 1963, pp. 519–525.
doi:10.1115/1.3656897

[27] Tanaka, K., "Fatigue Crack Propagation from a Crack Inclined to the Cyclic Tension Axis," *Engineering Fracture Mechanics*, Vol. 5, 1974, pp. 594–507.